

Primary, Secondary, Tertiary and Quaternary Structure Levels in Linear Polysaccharides: From Random Coil, to Single Helix to Supramolecular Assembly

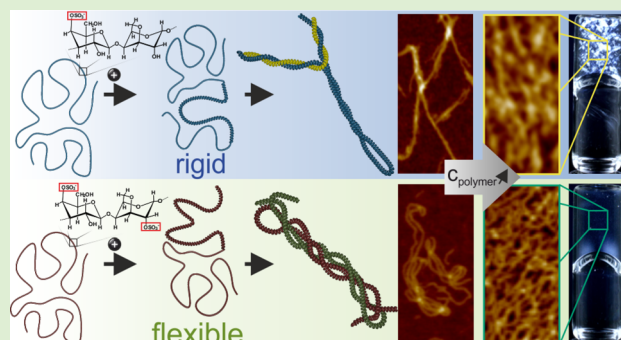
Michael Diener,^{†,ID} Jozef Adamcik,[†] Antoni Sánchez-Ferrer,^{†,ID} Florian Jaedig,[†] Larissa Schefer,[†] and Raffaele Mezzenga^{*,‡,§,ID}

[†]Department of Health Sciences and Technology, ETH Zürich, 8092 Zürich, Switzerland

[‡]Department of Materials, ETH Zürich, 8093 Zürich, Switzerland

Supporting Information

ABSTRACT: Polysaccharides are ubiquitous in nature and represent an essential class of biopolymers with multiple levels of conformation and structural hierarchy. However, a standardized structural nomenclature, as in the case of proteins, is still lacking due to uncertainty on their hierarchical organization. In this work we use carrageenans as model polysaccharides to demonstrate that several structural levels exist and can be unambiguously resolved by statistical analysis on high resolution Atomic Force Microscopy images, supported by spectroscopic, X-ray scattering and rheological techniques. In direct analogy with proteins, we identify primary, secondary, tertiary and quaternary structures. The structure–property relationship induced by monovalent ions for κ -, ι - and the non-gelling control λ -carrageenan is established from the single chain regime to the occurrence of hydrogels at higher concentrations. For κ -carrageenan in the presence of potassium, a disorder–order transition from random coil to single helix is first observed (secondary structure), followed by intrachain supercoiling events (tertiary structure) and macroscopic anisotropic domains which are parts of a network (quaternary structure) with tunable elasticity up to $\sim 10^3$ Pa. In contrast, κ -carrageenan in the presence of sodium only produces changes in secondary structure without supercoiling events, prior to formation of gels, highlighting the ion-specificity of the process. Loosely intertwined single helices are observed for ι -carrageenan in the presence of sodium and potassium chloride, providing an elastic mesh with many junction zones, while λ -carrageenan does not undergo any structural change. A generality of the observed behavior may be inferred by extending these observations to a distinct class of polysaccharides, the weak carboxylic polyelectrolyte Gellan gum. These results advance our understanding of ion-specific structural changes of polysaccharides and the physical mechanisms responsible for their gelation.



INTRODUCTION

Polysaccharides are abundant and widespread biopolymers that exhibit organized and semiorganized heterogeneous assemblies fulfilling a multitude of functions including cellular support, communication and energy storage.¹ Many of these natural polysaccharides form, under specific conditions, a continuous network gel connected either by chemical or physical bonds. The latter are prevalent in biopolymers experiencing a subtle interplay between solvent interaction and aggregation, which ultimately rules the overall gelation mechanism.² The molecular structure, nature of the counterion, polymer concentration and temperature are additional crucial parameters.^{3–5} The interactions involved in the formation of physical gels are non-covalent bonds such as hydrogen bonds, hydrophobic interactions and ionic complexes stabilizing the junction zones.^{2,6} Carrageenans are an illustrative example of commercially available, algal, sulfated, linear polysaccharides with a galactan backbone. They are well-known for their

gelling, thickening and stabilizing properties and thus widely used in the food, medical, cosmetic and pharmaceutical industry.⁷ The three main carrageenan families are named κ -, ι - and λ -carrageenan, classified according to the increase in linear charge density with one, two and three sulfate groups per ideal disaccharide subunit, respectively. Ion-specific gelation is generally observed in two varieties, κ - and ι -carrageenan, as studied by optical,⁸ mechanical,^{9–11} thermal and electromagnetic techniques.^{12,13} Although generally a non-gelling polysaccharide, λ -carrageenan has been shown to form gels in the presence of trivalent ions.¹⁴ From some of these studies, it was concluded that the gelation efficiency follows a distinct order for different cations.^{3,12,15} However, the molecular gelation mechanism of carrageenans has been a matter of

Received: January 18, 2019

Revised: February 16, 2019

Published: February 28, 2019

debate over the past decades due to inconsistent experimental evidence from scattering,^{4,16} spectroscopic,^{3,17} thermal,^{10,11,18} rheological^{3,18–20} and microscopic techniques.^{18,21} Multiple models were postulated including the double helical model,²² the Domain model^{3,23} and cation-mediated single helix aggregation.^{24,25} The fibrous model indicates supercoiling of double helices forming helical dimers further aggregating to form superstrands.^{8,26} Recently, by using high resolution AFM imaging in dilute conditions, the early assembly state was successfully resolved to be constituted by unimeric single helices formed via a coil–helix transition starting from individual polymer chains in random coil conformation,²⁷ followed by further assembly into supramolecular multi-filamented structures reminiscent of coiled-coil aggregates in proteins.²⁸ Remarkably, when divalent and trivalent iron ions were used as secondary structure triggering ions, the conformation of the single chains could even be manipulated by external magnetic fields.²⁹

In this work, we provide compelling evidence of ion-mediated primary, secondary, tertiary and quaternary structures in at least two families of carrageenans by using single molecule imaging and statistical polymer physics analysis on high resolution AFM images, supported by spectroscopic, X-ray scattering and rheological techniques. This allow us to present a refined definition of the structure hierarchy present in assembling polysaccharides, in direct analogy with the well-known and established protein nomenclature, and to provide the basis for understanding the physical gelation mechanisms of these biopolymers.

MATERIALS AND METHODS

Materials. κ - (CAS 11114-20-8, lot no. 1432063), ι - (type II, CAS 9062-07-1, lot no. 021M1764 V), λ -carrageenan (CAS 9064-57-7, lot no. 1408463 V) and potassium chloride ($\geq 99.9\%$, lot no. BCBP9964 V) were purchased from Sigma-Aldrich and analyzed (Table S1, Figure S1 S2). Molecular weights of 11.8 kDa and 201.0 kDa were calculated for κ - and ι -carrageenan, respectively. Sodium chloride (CAS 7440-23-5, lot no. K43132604207) was obtained from Merck. Ultrapure water (18.2 MΩ·cm at 25 °C) was acquired from a Milli-Q integral water purification system (Millipore Corporation). (3-Aminopropyl)triethoxysilane (APTES, CAS 919-30-2, 99.9%) for mica modification was purchased from Sigma-Aldrich. Dialysis membranes (7 Spectra/Por standard grade dialysis tubing, regenerated cellulose, 50 kDa MWCO) were purchased from Spectrum Laboratories.

Methods. Sample Preparation and Purification. The purchased carrageenan powders were used without any further purification except if indicated. For gelation experiments, aqueous carrageenan solutions were prepared by dissolving the powder at 90 °C for 60 min while constantly shaking. Corresponding salt solutions were added to the polymer solutions while vortexing to reach 0.5 wt % in polysaccharide and ionic strengths from 0 to 100 mM. Further experiments were performed after equilibration for at least 24 h at room temperature. Selected gelated samples were quenched with liquid nitrogen and then lyophilized for at least 24 h (with a LSL Secfroid) prior to X-ray scattering experiments.

In order to obtain ionic purified samples for gelation experiments, the ionic purification with ion exchange was conducted according to the protocol established by Schefer et al.^{27–30} Stock solutions of 0.25 wt % of each carrageenan type were obtained by dissolving the powder in Milli-Q for 60 min at 90 °C, while constantly shaking, and equilibrating overnight at ambient temperature to achieve complete dissolution. The stock solutions were purified by dialysing against Milli-Q changing the water bath after 2, 4 and 8 h to remove excess salts. Carrageenans were then transformed to their Na- or K-form by ion-exchange, changing the bath after 24, 26, 28 and 32 h. Any excess

ions from the ion exchange were removed by performing another dialysis step against Milli-Q water with bath changes after 48, 50, 52, 56 h and terminating the process after 72 h in total. The polymer concentration was determined by Optical Rotatory Dispersion (ORD) based on a linear regression of carrageenan calibration solutions with defined concentrations. The purified carrageenan solution was concentrated by pointing a constant, filtered 0.1 mPa air flow to the solutions interface while being constantly stirred. The final polymer concentration was determined from the weight loss, assuming solely water evaporation during the process. To obtain samples with a polymer concentration of 0.5 wt %, salt solutions of the desired cation were added while vortexing to reach ionic strengths ranging from 0 to 100 Mn.

Techniques. AFM Sample Preparation and Imaging. The same protocol as in previous studies^{27–30} was used to prepare the AFM samples by first modifying freshly cleaved mica with an aqueous APTES solution to obtain a positive surface charge. 20 μL of sample in sol state or a spoon-full of gelled sample was adsorbed for 30 s, dropwise rinsed with 1 mL of Milli-Q water and gently dried with pressurized air. The surface was probed using a Nanoscope VIII Multimode Scanning Force Microscope (Bruker AXS) with commercial silicon nitride cantilevers in tapping mode under ambient conditions. A third order flattening to remove background curvature was used on all the AFM images, and no further image processing was conducted.

Rheological Measurements. The rheological measurements were performed on a Physica MCR 501 (Anton Paar, Graz, Austria) equipped with a CP25-2 cone plate geometry and a double gap DG 27.9 for gelled samples and solutions, respectively. Samples were transferred directly with a micropipette or a spoon, depending on the viscosity. A solvent trap was used to minimize solvent evaporation and the temperature was kept constant at 25 °C. The linear viscoelastic regime was determined in a strain sweep from 0.1 to 100% at an angular frequency of 1 rad/s. Subsequent frequency sweeps from 0.1 to 100 rad/s were performed at 1% strain.

WAXS Measurements. Wide-angle X-ray scattering experiments were performed using a Rigaku MicroMax-002+ microfocused beam (40 W, 45 kV, 0.88 mA) with the $\lambda_{\text{CuK}\alpha} = 0.15418 \text{ nm}$ radiation in order to obtain direct information on the scattering patterns. The scattering intensities were collected by a Fujifilm BAS-MS 2025 imaging plate system (15.2 cm × 15.2 cm, 50 μm resolution). An effective scattering vector range of $0.05 \text{ nm}^{-1} < q < 25 \text{ nm}^{-1}$ was obtained, where q is the scattering wave vector defined as $q = 4\pi \sin \theta / \lambda_{\text{CuK}\alpha}$ with a scattering angle of 2θ .

RESULTS

Ion-Specific Secondary Structure Formation in Carrageenan. The ion-specific coil-to-helix transition of κ -carrageenan^{28,30} was followed on a single molecular level by polymer statistical analysis (Figure 1). A pure phenomenological approach was followed by comparing the occurrence of κ -carrageenan in its primary and its secondary conformation in various ionic concentrations of sodium and potassium chloride in order to get a quantitative measure for the ion-specific secondary structure formation in the dilute regime. In order to estimate the influence of each specific cation, Na^+ and K^+ , κ -carrageenan was purified and transformed to the corresponding salt form.²⁸ AFM height images of representative polysaccharide chains of each population at low polymer concentration (Figure 1A,B) were traced with “FiberApp”,³¹ and the height histograms of each population were compared (Figure 1C,D). The measured height of the primary structure is around $0.2 \pm 0.1 \text{ nm}$, whereas the single helices are at $0.5 \pm 0.1 \text{ nm}$, matching the previously published data from purified samples.^{27–30} The ratios of random coil to single helical fractions are plotted as a function of ionic strength (Figure 1E), and monotonically increasing curves for both cations, i.e.,

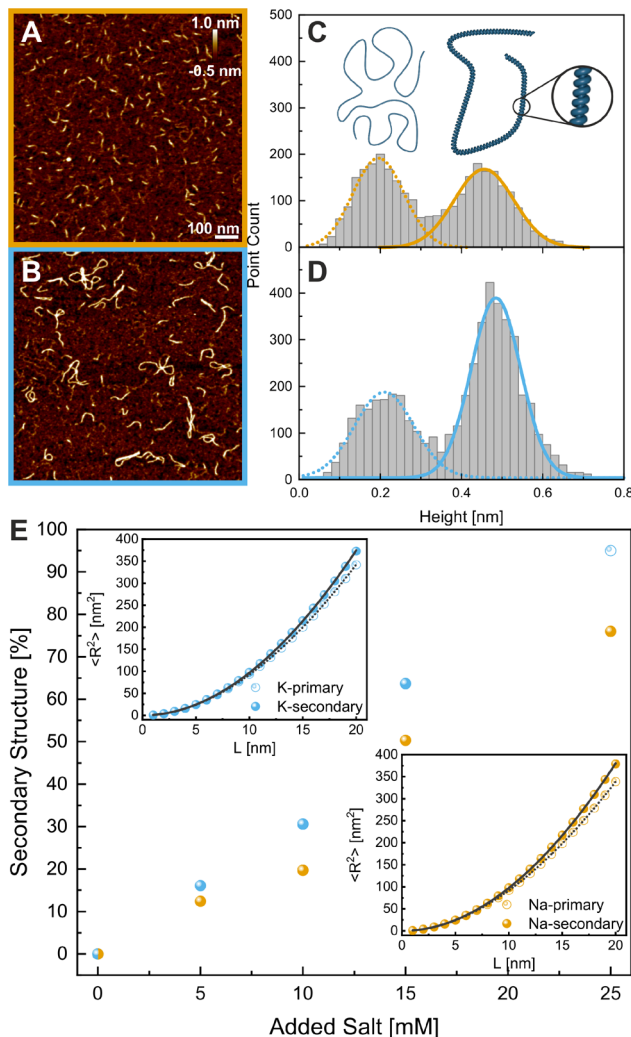


Figure 1. AFM height images of purified κ -carrageenan at 1 $\mu\text{g}/\text{mL}$ with 15 mM of sodium and potassium chloride added, respectively (A, B). Scale and height bar corresponds to both images. Height histograms with Gaussian fits of tracked polymer chains revealing different ratios of primary (dashed) and secondary structure (solid) in 15 mM of (C) sodium and (D) potassium chloride. Conversion rate of primary to secondary structure upon the addition of sodium (orange) and potassium (blue) chloride as calculated by the ratio of area of histograms, normalized to the maximum conversion for K^+ approximated (hollow dot) (E). Insets represent mean-square end-to-end distances versus internal contour length for primary (empty) and secondary (full) conformation with 2D Worm-Like Chain (WLC) fits.

Na^+ and K^+ , are observed, with a clear trend toward more secondary structures formation in the presence of potassium, indicating an enhanced binding affinity of these cations to κ -carrageenan. Theoretical maximum conversion of chains to secondary or higher order structures was observed at 25 mM KCl making a tracing and statistical analysis of fibers chains for polymer statistical analysis impossible due to the occurrence of tertiary and quaternary structures. Thus, maximal conversion was approximated as indicated by the hollow data point in Figure 1E. Upon the addition of sodium chloride, no tertiary or quaternary structures were observed and the maximum conversion was reached at 100 mM and higher.³⁰ In order to quantify the flexibility of the single polymer chains, the mean-square end-to-end distance of each population was fitted to extract the persistence length of either random coil or helical

conformations, revealing the stiffening of the polymer from $19.2 \pm 0.1 \text{ nm}$ to $66.4 \pm 3.2 \text{ nm}$ and $20.5 \pm 0.4 \text{ nm}$ to $50.0 \pm 2.7 \text{ nm}$ for sodium and potassium chloride, respectively. This more than doubling in persistence length is only observable in κ - while ι -carrageenan forms much more flexible single helices reaching persistence lengths of maximum 30.0 nm.³⁰

Ion-Induced Tertiary and Quaternary Structure Formation in Carrageenan.

The ion-induced single helices form more complex structures at further increasing salt concentrations. Two different hierarchy levels of assemblies, intramolecular and intermolecular, were differentiable on AFM height images (Figures 2 and S3 and S4). As all AFM

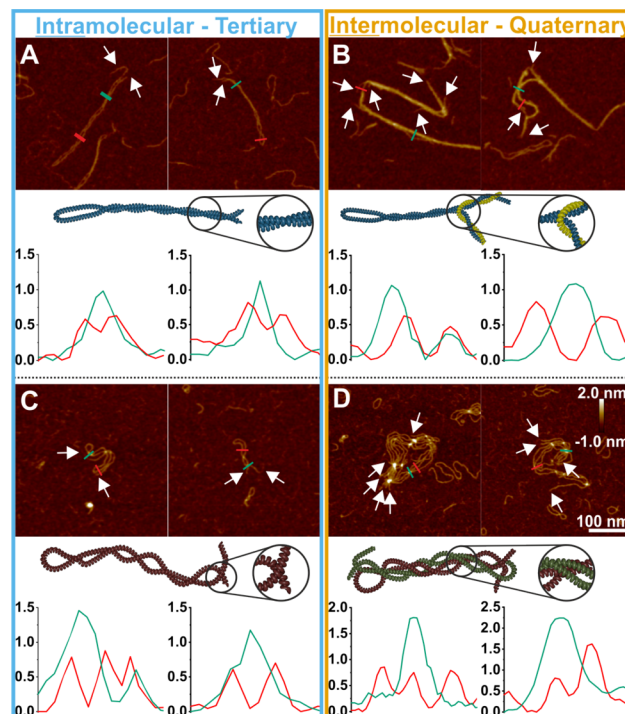


Figure 2. Representative AFM height images with corresponding height profiles of selected cross sections in nm for (A, C) intramolecular–tertiary and (B, D) intermolecular–quaternary assemblies. (A, B) show structures in the case of rigid secondary structures, whereas (C, D) shows the flexible molecules coiling pathways. White arrows point to endings of the polymer chain(s).

measurements were obtained on dried specimens to get high resolution images, control experiments in liquid were performed to prove that the drying process does not induce structural assembly of polysaccharide chains (Figure S5). The simplest refers to intramolecular, intertwined structures with two endings from a single polysaccharide chain unambiguously identifiable, indicated by white arrows in Figure 2 and accompanied by hairpin loops, and categorized as tertiary structures, since this structure involves a single chain (and two chains ends). Thus, tertiary structures observed here are reminiscent of supercoiled DNA, with the main difference that supercoiling in these polysaccharides occurs among portions of the same chain having turned to single helix (and not double helix as in DNA). The height profiles also reveal a doubling in height up to 1.2 nm, indicating that these structures consist of two single helices (from the same chain) coiling, overlapping or laterally aggregating. Increased height values along a major part of the contour was observed for more rigid object (Figure

2A), whereas only several overlapping points were identified in flexible molecules (Figure 2C).

As soon as multiple polymer chains are involved, the structures increase in complexity due to branching, lateral aggregation events and coiled-coil interactions (Figure 2B,D). The height profiles reveal values greater than the height of a single helix, reaching up to 2.0 nm. However, the main difference to tertiary structures is that multiple chain ends are visible, demonstrating the involvement of two or more polymer chains in these assemblies, therefore referred to as quaternary structures.

Macroscopic Properties and Rheology of Hydrogels.

The primary, chemical structures of the three investigated sulfated polysaccharides differ in the linear charge density of their ideal subunit, as well as the absence of the 3,6-anhydro-bridge in λ -carrageenan (Figure 3C,F,I). This structural

domains in the similar length scale range. This cooperative ordered state, inferring nematic gels, has been reported numerous times for rigid objects such as tobacco mosaic virus,³³ amyloid fibrils^{34,35} and nanocrystalline cellulose,³⁶ and is typical of rigid objects with a high aspect ratio oriented by a common field director. The only known reports of nematic phases in carrageenans are for sonicated κ -carrageenan in the presence of potassium iodide, where the iodide are meant to inhibit the aggregation of rigid helices;^{37,38} to the best of our knowledge, this is the first report where nematic gels are observed in the presence of chloride counterions. ι -carrageenan solutions show the same birefringence as the ones for κ -carrageenan with sodium chloride, whereas λ -carrageenan solutions did not reveal any birefringence, neither in the presence of NaCl nor of KCl.

Rheological measurements provide further insights into the ion-induced sol–gel transition. For the κ - and λ -polymer solutions in the native state, the viscous components, G'' , are of 1 order of magnitude higher than the elastic ones, G' , with slopes of value 1 (Figure 3B,H), typical of polymer solutions. ι -carrageenan shows a different behavior compared to κ - and λ -carrageenan, as the system was jammed already without salt addition (Figure 3D,E). A plausible explanation is that residual cations present in the commercial powder are inducing the formation of secondary and higher hierarchical structures whereas purified solutions show a frequency dependence typical of polymer solutions (Table S1 and Figure S6). Upon the addition of salt, a continuous gel network is formed as indicated by the frequency independent storage and loss moduli. The storage and loss moduli have a difference of at least 1 order of magnitude as expected for strong gels. The network elasticity G_0 , defined by the plateau modulus G' at 10 rad/s, varied a lot depending on the type of carrageenan and the cation added. The elasticity is tunable over several orders of magnitude by adding different amounts of salt, reaching up to 1.4×10^3 Pa for κ -carrageenan with potassium chloride, again demonstrating the ion-specificity of κ -carrageenan for potassium. Similar values and behavior were reported previously.^{21,39} The addition of salt to ι -carrageenan solutions did not show a drastic change in the rheological curves as the native polysaccharide solution alone already showed a frequency independence, characteristic for gelled systems. The addition of sodium chloride to ι -carrageenan led to a higher elasticity of 1.5×10^1 Pa compared to 4.2×10^0 Pa with the addition of potassium chloride. The two gelling carrageenan species showed distinct flow behavior in rotational experiments as in κ -carrageenan the elastic components started to drop at 1% strain compared to ι -carrageenan at 15%, being characteristic for brittle and elastic networks, respectively (Figure 3C,F,I).

Molecular Assembly of Network Building Blocks.

AFM imaging was performed in order to further elucidate the molecular assembly and bridge the gap between molecular assembly and macroscopic properties.

Figure 4A depicts the approach of first scanning regions far away from the spot of interest, first obtaining images in pseudosemidilute regions to visualize the structure and the arrangement of single chains, as shown in the sequence of Figure 4B–D. Moving toward the center to more concentrated and packed areas, one can observe the real structure within the network revealing mesoscopic characteristics. The denser the molecules pack, the less visible the individual chains are in the height channel; in the amplitude mode, they are, however, still

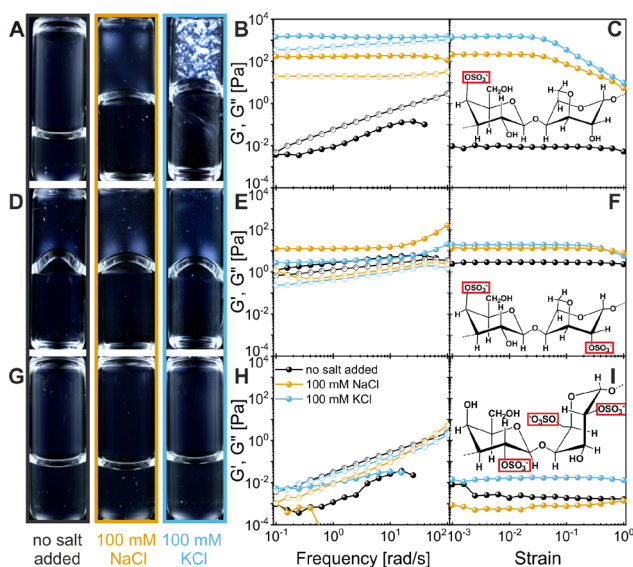


Figure 3. (A) κ -, (D) ι - and (G) λ -carrageenan solutions at 0.5 wt % with different added chloride salts placed between cross-polarizers in order to show the birefringence and turned upside down to visualize the solid-like behavior upon gelation. Storage G' (full symbols) and loss G'' (empty symbols) moduli at 1% strain as a function of angular frequency for (B) κ -, (E) ι - and (H) λ -carrageenan. Storage modulus G' at 1 rad/s for 0.1 to 100% strain for (C) κ -, (F) ι - and (I) λ -carrageenan. Legend applies to all rheology graphs. Chemical structure of the ideal subunit of (C) κ -, (F) ι - and (I) λ -carrageenan with the sulfate group framed.

difference induces kinks in the primary structure of λ -carrageenan preventing the formation of secondary structures, and thus no gelation upon addition of mono- or divalent cations occurs.³² Indeed, also in the present case, λ -carrageenan shows neither sol–gel transition nor birefringence upon the addition of the investigated monovalent ions. The transition from sol to gel is obvious in the case of κ -carrageenan, as the commercial polymer solution without any additional salt clearly did not withstand gravitational forces when turned upside down, whereas the ones with added salt did (Figure 3A). Solutions of κ -carrageenan with sodium show a weak, homogeneous loom between cross-polarizers, implying a uniform structure on the submicron scale, while the heterogeneous pattern with bright and dark regions in the presence of potassium indicates variations in the interaction with visible light caused by the occurrence of spatially ordered

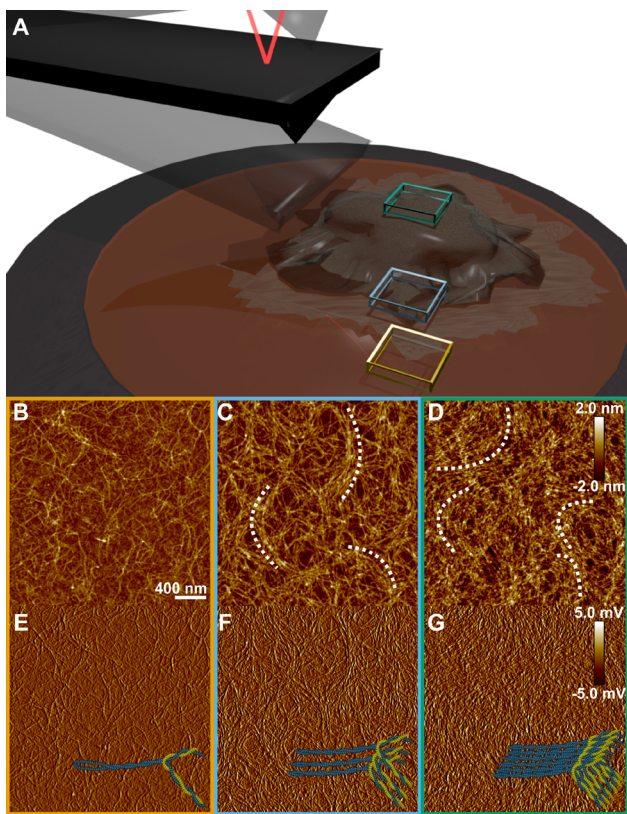


Figure 4. (A) Schematic of the experimental AFM setup showing different regions probed, starting scanning from the peripheries of the gel moving inward to denser areas. AFM height (B, C, D) and amplitude (E, F, G) images of 0.5 wt % κ -carrageenan gels with 100 mM KCl, in the corresponding regions of interest as shown in (A) revealing variations in packing of the single polysaccharide chains yielding ordered domains. Inset model of self-assembled polymer chains, as well as dotted line help to guide the eye to visualize structure and the orientation present in the gel network. Scale bars applies to all images.

distinguishable (Figure 4E–G). In the case of κ -carrageenan with potassium chloride, the rigid tertiary and quaternary structures form a continuous network based on branching and lateral aggregation, as previously described in dilute, purified samples (Figure S7).²⁸ These distinguishable, individual clusters, ultimately forming an infinite network, percolate through the entire volume providing the measured bulk elasticity.^{40–42} Polymers in secondary structure state among tertiary and quaternary structures are observable in the outer regions, indicating a slight microphase separation explainable by the syneresis effect.^{21,41} As indicated by the inset sketches, the packing of the tertiary and quaternary structures is suggested to give rise to ordered domains of several hundreds of nanometres in size, explaining the distinct chirooptical property of κ -carrageenan hydrogels induced by potassium ions previously described (Figure 3A).

Entangled polymer chains with segments in secondary state were observed in the case of commercial κ -carrageenan, explainable by the residual cation composition present in the powder (Figures 5A and S7). The absence of ordered assemblies and continuous structures give rise to the macroscopic sol properties previously explained. When sodium or potassium chloride is added, the typical sol–gel transition is detected and a change in structure can be observed as single

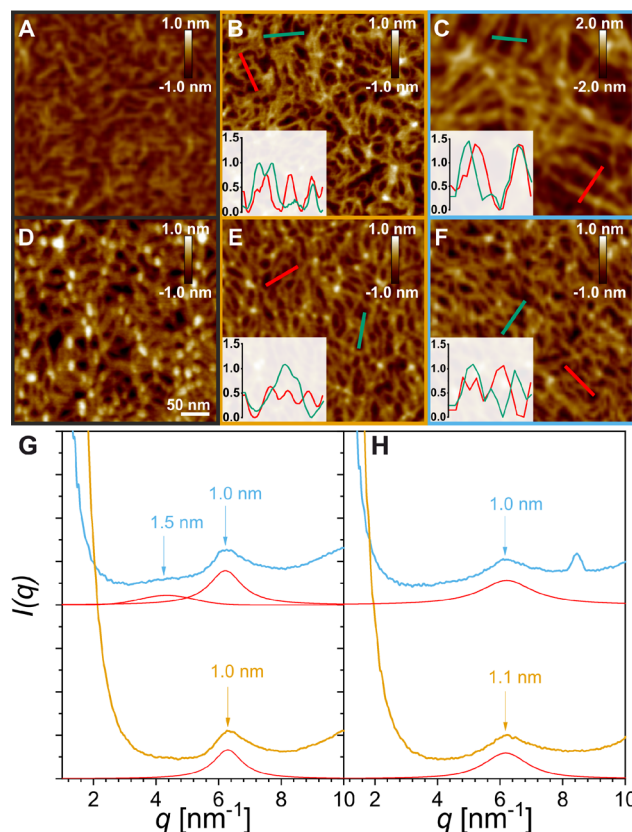


Figure 5. AFM height images for 0.5 wt % κ - and ι -carrageenan solutions without any additional salt (A, D), with 100 mM NaCl (B, E) and KCl (C, F) added. Insets show relative height profiles of corresponding colored lines in AFM height images. Scale bar applies to all images. 1D WAXS intensity profile with the corresponding deconvoluted peaks for the secondary structure features of lyophilized (G) κ - and (H) ι -carrageenan solutions with added 100 mM of sodium (orange) and potassium (blue) chloride.

helices are formed, allowing for the formation of tertiary and quaternary structures, and thus additional junction zones. A characteristic reflection at $q = 6.2 \text{ nm}^{-1}$ occurs in the 1D WAXS intensity profile of both κ - and ι -carrageenan exposed to sodium and potassium salts which can be attributed to the interdistance between single helices, as confirmed by the absence of such a peak in the non-helix-forming λ -carrageenan (Figures 5G,H, S9, S10 and S11). In the case of ι -carrageenan, an infinite network is observed already in the case without any salt addition. Upon the addition of monovalent sodium and potassium chloride salts, tertiary and mainly quaternary structures dominate, with distinguishable loosely intertwined single helices of 1.0 nm height maximum (Figure 5E,F). This fine mesh of entangled polysaccharide helices and their numerous junction zones provide the characteristic deformability (Figure 3F). As already presented in Figure 4, the addition of potassium chloride to κ -carrageenan leads to unique optical and mechanical properties, which can be explained by the microstructures observable by AFM. The ion-induced single helices follow the suggested pathway of the fibrous model²⁸ by laterally aggregating and branching to form rigid superstrands of 1.5 nm height composing a continuous, percolating network. Remarkably, analyzing the WAXS profiles of potassium induced hydrogels, a shoulder at $q = 4.3 \text{ nm}^{-1}$ appears, reflecting these unique tight tertiary and quaternary structures with structural features of 1.5 nm, in agreement with

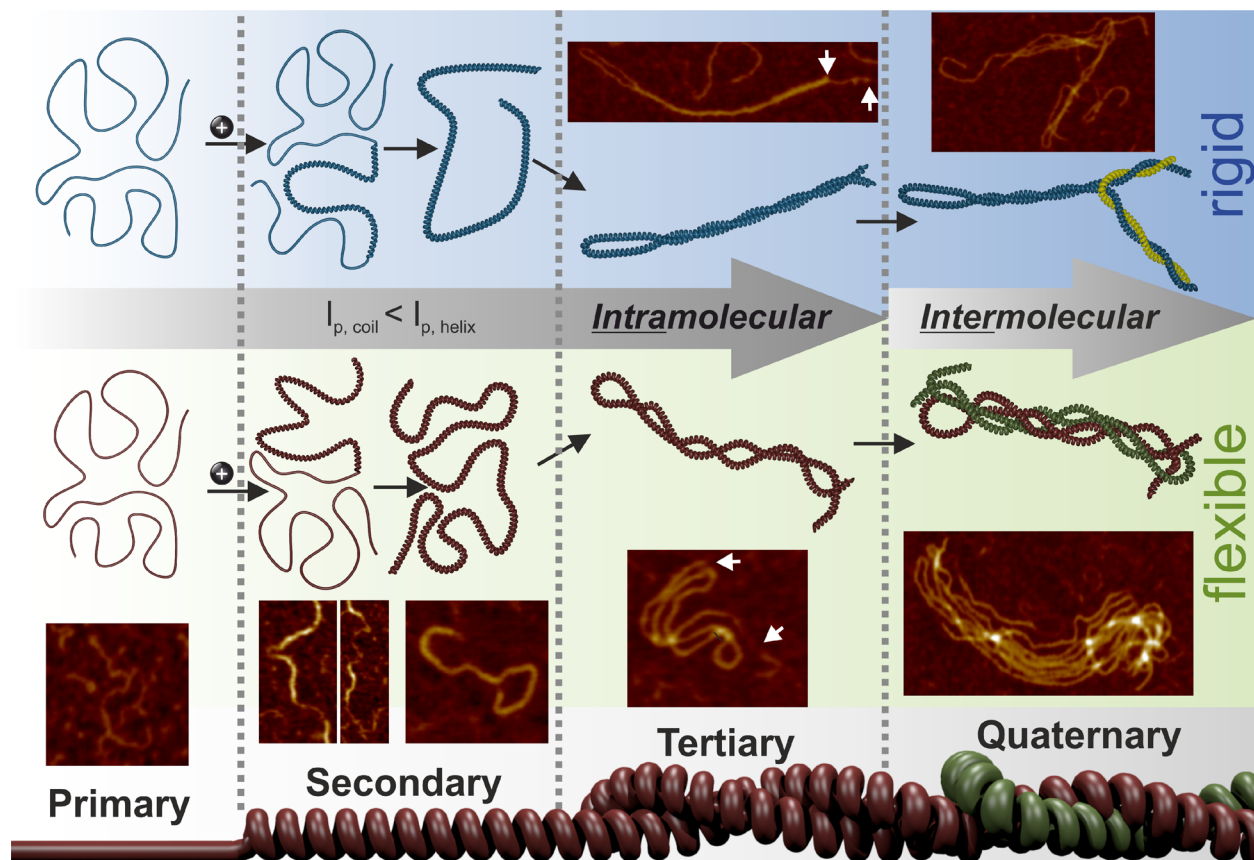


Figure 6. Schematic elucidation of the adaptation of the protein nomenclature to the different ion-induced structures in a linear charged polysaccharide from primary to quaternary level with representative AFM height images. Primary structure is defined as the sequence of sugar monomers in random coil conformation, then forming intramolecular single helices with different persistence lengths as secondary structure. Tertiary structure sees a variety of conformations ranging from tight to loosely supercoiled helices. Intermolecular quaternary structure shows both tightly or loosely intertwined tertiary structures of like-chains from distinct polymers, the simplest form of which is reminiscent of coiled-coil structures in proteins and polypeptides.

the AFM imaging (Figure 5C). This side-by-side association increases the cross-link points in the system causing branching of the network, which was reported before,^{43,44} and which percolates through the entire gel.⁴² In support of this picture, the scaling exponent of the power-law expressing the elastic modulus versus ε , the relative distance (in composition) from the gelling point, is found to obey the percolation theory $G_e \propto \varepsilon^{2.2}$, in line with de Gennes prediction of $G_e \propto \varepsilon^{1.9}$.^{10,45}

■ DISCUSSION

Conformational Nomenclature. Macromolecules such as polypeptides or polysaccharides are characterized by multiple structural levels, creating the need for a nomenclature. The terms established for protein as primary, secondary, tertiary and quaternary structure have been previously also used to characterize polysaccharide structure hierarchy,^{3,6,46,47} but they suffered from the major drawback of *hl*/understating the first ordered state of a single helix (secondary structure), which only recently has been conclusively determined.²⁷ In the present work, the structural diversity is characterized by four different levels built on each other, taking single helices as a fundamental first ordered state into account (Figure 6). This allows one to describe not only the conformational changes occurring in polysaccharides on a single molecular level but also their intra- and intermolecular interaction, network formation, clusters and aggregates in the concentrated regime.

The primary structure, as inspired from protein science, and previously defined, is the sequence of covalently linked monomers following a simple repeating pattern leading to homo- or copolymer chains. Besides the effective sequence of monomers, the primary structure in polysaccharides is defined by the variation of sugar monomers including different ring sizes and their absolute configuration (D or L), their points of linkage of the glycosidic bond, e.g., (1 → 4) or (1 → 6) and their anomeric configuration (α or β). The most relevant polysaccharides consist of pyranose rings, linked axially or equatorially with a glycosidic bond at different carbons in the monosaccharide unit. The primary structure of the polysaccharide chains occurs in random coil conformation, thereby characterized by specific but low persistence lengths, always far below their contour length and conferring to the chain a self-avoiding random walk chain statistics.^{30,48–50}

The most commonly formed secondary structures in proteins, α -helices and β -sheets, result due to the intra- and interchain hydrogen bonding along the amino acid peptide backbone, whereas in nucleic acids it is the intermolecular base pairing driven by hydrogen bonding, $\pi-\pi$ stacking and hydrophobic interactions forming an intermolecular double helix. Differently in polysaccharides, the secondary structure is defined by the intramolecular, regular, spatial arrangement of the primary sequence into a single helix.⁵¹ The linkage conformation, described by a set of dihedral angles of the

glycosidic bonds and repeating itself from residue to residue, gives rise to the helical secondary structure adopted by the polysaccharide chain.^{51,52} The helices form at any point along the chain, leading to single chains with coil and helix portions coexisting in a mixed way within the same chain. This disorder-order conformational transition, from coil to helix, induces local chirality, as well as an increase in chain rigidity.³⁰

The next higher structural level proved to be a point of high debate in previous studies, as in biopolymer gels, the distinction between pairwise association of single helices and intertwined double helices (as in DNA) appeared to be difficult to assess. Hence, the term helical dimer was often used.⁵³ Nevertheless, efforts were made to define these tertiary structures, resulting in various definitions, including non-covalent association between like-chains,^{46,47} homotypic intermolecular assemblies such as double helices⁶ or intermolecular association within domains of associated double helices.²³ All of these definitions omit the ordered state of a single helix as secondary structure and, unlike in the case of protein, intermolecular structures among distinct chains were considered tertiary structures. Thus, we can now establish a refined picture of tertiary structures as non-covalently linked intramolecular assemblies from portions of the same polymer chain already in their ordered (secondary) state. Depending on the flexibility of the secondary structure, either rigid, tightly intertwined supercoils or loosely overlapping and twisted structures are formed by rigid or flexible single helices, respectively. These tertiary structures are reminiscent of an old-fashioned supercoiled telephone cord, show features of hairpin loops and hairpin turns.

In previous studies, only synergistic interactions between distinct, unlike chains were considered quaternary structures.^{6,47} Again, as the single helix was not considered as the fundamentally ordered state, the quaternary structures can now be redefined as following. The non-covalent association of these unimeric tertiary structures between like-chains or the intermolecular twisting of secondary structures from distinct chains leads to the formation of the so-defined quaternary structures. In this way, side-by-side aggregation, end-to-end association, as well as branching become possible, enabling the formation of continuous three-dimensional networks. Furthermore, it is possible to identify the simplest form of quaternary structure as coiled single helices further twisting into each other as quaternary structure (Figure 6), reminiscent of coiled-coil conformation in proteins and polypeptides.

Interestingly, while the classification from primary to quaternary structures results equally suited for both polysaccharides and proteins, some major differences should be highlighted between these two classes of biopolymers. The main one is that while in the protein case, primary, secondary and tertiary structure always lead to a precise, deterministic, self-folding process providing a unique folded structure of the protein which remains identical from protein to protein, in the case of polysaccharides the ion-promoted folding events chain from primary to tertiary structures is a stochastic process, and thus it leads to virtually different configurations in each folding event. The same considerations can be extended for both classes of biopolymers to their quaternary structure.

To summarize, we have combined high resolution AFM imaging, statistical polymer physics, X-ray scattering, rheology and spectroscopic techniques to resolve all the hierarchical degrees of structure of ion-binding carrageenan polysaccharides. This has allowed us to provide a refined nomenclature to

identify the various structural levels, from primary to quaternary structure, in full analogy with protein structural identification, and to lay the foundation for the understanding of their gelling behavior. At the single molecular level and for high enough concentrations, κ -carrageenan in the presence of potassium ions forms single helices (secondary structure), further folding into single-chain supercoiled strands (tertiary structure) and then side-by-side rigid superstrands with other chains (quaternary structure), the simplest form of which is coiled-coil helices. This ultimately leads to the formation of an infinite, branched supramolecular physical network with local anisotropic orientation. The ion-specificity is quantified by comparing the ratio of polymer chain populations in primary and secondary state based on statistical analysis of AFM height images. In contrast to κ -carrageenan, ι -carrageenan forms a more flexible network upon the addition of sodium, which is solely composed of aggregating single helices, i.e., without notable tertiary structure. Although the main focus of this study was the investigation of the ion-induced hierarchical assembly and gelation mechanisms of carrageenans, the results presented here may bear a general relevance. Indeed, Gellan gum, another example of linear anionic polysaccharide (yet a weak carboxylic polyelectrolyte, as opposed to the strong sulfate polyelectrolytes given by the carrageenans), shows similar feature as for the ion-induced secondary, tertiary and quaternary structures, as shown in Figure S12. Furthermore, the same two-step ion-induced gelation mechanism is also observed for this system (see Figure S13), inferring a general mechanism common to more than one single class of polysaccharides.

ASSOCIATED CONTENT

S Supporting Information

The Supporting Information is available free of charge on the ACS Publications website at DOI: [10.1021/acs.biomac.9b00087](https://doi.org/10.1021/acs.biomac.9b00087).

Additional details ([PDF](#))

AUTHOR INFORMATION

Corresponding Author

*R. Mezzenga. E-mail: raffaele.mezzenga@hest.ehtz.ch.

ORCID

Michael Diener: [0000-0003-0919-9434](https://orcid.org/0000-0003-0919-9434)

Antoni Sánchez-Ferrer: [0000-0002-1041-0324](https://orcid.org/0000-0002-1041-0324)

Raffaele Mezzenga: [0000-0002-5739-2610](https://orcid.org/0000-0002-5739-2610)

Notes

The authors declare no competing financial interest.

ACKNOWLEDGMENTS

We thank Christoph Zeder for performing Flame-AAS experiments, Peter Fischer and Pascal Bertsch for granting access to the rheometer and for their valuable inputs.

REFERENCES

- (1) Sletmoen, M.; Maurstad, G.; Sikorski, P.; Paulsen, B. S.; Stokke, B. T. Characterisation of Bacterial Polysaccharides: Steps towards Single-Molecular Studies. *Carbohydr. Res.* **2003**, *338*, 2459–2475.
- (2) Djabourov, M.; Nishinari, K.; Ross-Murphy, S. B. *Physical Gels from Biological and Synthetic Polymers*; Cambridge University Press: Cambridge, 2013.

- (3) Morris, E. R.; Rees, D. A.; Robinson, G. Cation-Specific Aggregation of Carrageenan Helices: Domain Model of Polymer Gel Structure. *J. Mol. Biol.* **1980**, *138*, 349–362.
- (4) Meunier, V.; Nicolai, T.; Durand, D. Structure of Aggregating Kappa-Carrageenan Fractions Studied by Light Scattering. *Int. J. Biol. Macromol.* **2001**, *28*, 157–65.
- (5) Mangione, M.; Giacomazza, D.; Bulone, D.; Martorana, V.; San Biagio, P. Thermoreversible Gelation of κ -Carrageenan: Relation between Conformational Transition and Aggregation. *Biophys. Chem.* **2003**, *104*, 95–105.
- (6) Eggleston, G.; Doyle, J. P. Polysaccharides: Molecules, Clusters, Networks, and Interactions. In *Advances in Biopolymers*; Fishman, M. L., Qi, P. X., Wicker, L., Eds.; ACS Symposium Series; American Chemical Society: Washington, DC, 2006; pp 19–34.
- (7) vande Velde, F.; De Ruiter, G. A.. Carrageenan. In *Biopolymers Online*; Vandamme, E. J., De Baets, S., Steinbüchel, A., Eds.; Wiley-VCH Verlag GmbH & Co. KGaA: Weinheim, Germany, 2005; pp 1–21.
- (8) Hermansson, A. M.; Eriksson, E.; Jordansson, E. Effects of Potassium, Sodium and Calcium on the Microstructure and Rheological Behaviour of Kappa-Carrageenan Gels. *Carbohydr. Polym.* **1991**, *16*, 297–320.
- (9) Piculell, L.; Nilsson, S.; Muhrbeck, P. Effects of Small Amounts of Kappa-Carrageenan on the Rheology of Aqueous Iota-Carrageenan. *Carbohydr. Polym.* **1992**, *18*, 199–208.
- (10) Liu, S.; Huang, S.; Li, L. Thermoreversible Gelation and Viscoelasticity of κ -Carrageenan Hydrogels. *J. Rheol. (Melville, NY, U.S.)* **2016**, *60*, 203–214.
- (11) Liu, S.; Li, L. Thermoreversible Gelation and Scaling Behavior of Ca²⁺-Induced κ -Carrageenan Hydrogels. *Food Hydrocolloids* **2016**, *61*, 793–800.
- (12) Zhang, W.; Piculell, L.; Nilsson, S.; Knutsen, S. H. Cation Specificity and Cation Binding to Low Sulfated Carrageenans. *Carbohydr. Polym.* **1994**, *23*, 105–110.
- (13) Nilsson, S.; Piculell, L. Helix-Coil Transitions of Ionic Polysaccharides Analyzed Within the Poisson-Boltzmann Cell Model. 4. Effects of site-specific counterion binding. *Macromolecules* **1991**, *24*, 3804–3811.
- (14) Running, C. A.; Falshaw, R.; Janaswamy, S. Trivalent Iron Induced Gelation in Lambda-Carrageenan. *Carbohydr. Polym.* **2012**, *87*, 2735–2739.
- (15) Michel, A.-S.; Mestdagh, M.; Axelos, M. Physico-Chemical Properties of Carrageenan Gels in Presence of Various Cations. *Int. J. Biol. Macromol.* **1997**, *21*, 195–200.
- (16) Croguennoc, P.; Meunier, V.; Durand, D.; Nicolai, T. Characterization of Semidilute κ -Carrageenan Solutions. *Macromolecules* **2000**, *33*, 7471–7474.
- (17) Bongaerts, K.; Reynaers, H.; Zanetti, F.; Paoletti, S. On the Molar Mass of κ -Carrageenan in the Course of Conformational Transition from the Disordered to the Fundamental Ordered Form. *Macromolecules* **1999**, *32*, 675–682.
- (18) Núñez-Santiago, M. d.C.; Tecante, A. Rheological and Calorimetric Study of the SolGel Transition of κ -Carrageenans. *Carbohydr. Polym.* **2007**, *69*, 763–773.
- (19) Pelletier, E.; Viebke, C.; Meadows, J.; Williams, P.a. Solution Rheology of κ -Carrageenan in the Ordered and Disordered Conformations. *Biomacromolecules* **2001**, *2*, 946–951.
- (20) Viebke, C.; Piculell, L.; Nilsson, S. On the Mechanism of Gelation of Helix-Forming Biopolymers. *Macromolecules* **1994**, *27*, 4160–4166.
- (21) Funami, T.; Noda, S.; Nakauma, M.; Ishihara, S.; Takahashi, R.; Al-Assaf, S.; Ikeda, S.; Nishinari, K.; Phillips, G. O. Molecular Structures of Gellan Gum Imaged with Atomic Force Microscopy in Relation to the Rheological Behavior in Aqueous Systems in the Presence or Absence of Various Cations. *J. Agric. Food Chem.* **2008**, *56*, 8609–8618.
- (22) Anderson, N. S.; Campbell, J. W.; Harding, M. M.; Rees, D. A.; Samuel, J. W. X-ray Diffraction Studies of Polysaccharide Sulphates: Double Helix Models for κ - and ι -Carrageenans. *J. Mol. Biol.* **1969**, *45*, 85–99.
- (23) Robinson, G.; Morris, E. R.; Rees, D. A. Role of Double Helices in Carrageenan Gelation: The Domain Model. *J. Chem. Soc., Chem. Commun.* **1980**, *0* (4), 152.
- (24) Smidsrød, O. Structure and Properties of Charged Polysaccharides. *27th Int. Congr. Pure Appl. Chem.* **1980**, 315–327.
- (25) Smidsrød, O.; Grasdalen, H. Some Physical Properties of Carrageenan in Solution and Gel State. *Carbohydr. Polym.* **1982**, *2*, 270–272.
- (26) Hermansson, A.-M. Rheological and Microstructural Evidence for Transient States During Gelation of Kappa-Carrageenan in the Presence of Potassium. *Carbohydr. Polym.* **1989**, *10*, 163–181.
- (27) Schefer, L.; Adamcik, J.; Mezzenga, R. Unravelling Secondary Structure Changes on Individual Anionic Polysaccharide Chains by Atomic Force Microscopy. *Angew. Chem., Int. Ed.* **2014**, *53*, 5376–5379.
- (28) Schefer, L.; Adamcik, J.; Diener, M.; Mezzenga, R. Supramolecular Chiral Self-Assembly and Supercooling Behavior of Carrageenans at Varying Salt Conditions. *Nanoscale* **2015**, *7*, 16182–16188.
- (29) Schefer, L.; Bulant, A.; Zeder, C.; Saha, A.; Mezzenga, R. Magnetic Control of Macromolecular Conformations in Supramolecular Anionic Polysaccharide-Iron Complexes. *Angew. Chem., Int. Ed.* **2015**, *54* (45), 13289.
- (30) Schefer, L.; Usov, I.; Mezzenga, R. Anomalous Stiffening and Ion-Induced Coil-Helix Transition of Carrageenans under Monovalent Salt Conditions. *Biomacromolecules* **2015**, *16*, 985–991.
- (31) Usov, I.; Mezzenga, R. FiberApp: An Open-Source Software for Tracking and Analyzing Polymers, Filaments, Biomacromolecules, and Fibrous Objects. *Macromolecules* **2015**, *48*, 1269–1280.
- (32) Rinaudo, M.; Karimian, A.; Milas, M. Polyelectrolyte Behavior of Carrageenans in Aqueous Solutions. *Biopolymers* **1979**, *18*, 1673–1683.
- (33) Fraden, S.; Maret, G.; Caspar, D. L.D.; Meyer, R. B. Isotropic-Nematic Phase Transition and Angular Correlations in Isotropic Suspensions of Tobacco Mosaic Virus. *Phys. Rev. Lett.* **1989**, *63*, 2068–2071.
- (34) Bolisetty, S.; Harnau, L.; Jung, J.-m.; Mezzenga, R. Gelation, Phase Behavior, and Dynamics of β -Lactoglobulin Amyloid Fibrils at Varying Concentrations and Ionic Strengths. *Biomacromolecules* **2012**, *13*, 3241–3252.
- (35) Nyström, G.; Arcari, M.; Mezzenga, R. Confinement-Induced Liquid Crystalline Transitions in Amyloid Fibril Cholesteric Tactoids. *Nat. Nanotechnol.* **2018**, *13*, 330–336.
- (36) Bertsch, P.; Isabettini, S.; Fischer, P. Ion-Induced Hydrogel Formation and Nematic Ordering of Nanocrystalline Cellulose Suspensions. *Biomacromolecules* **2017**, *18*, 4060–4066.
- (37) Borgström, J.; Piculell, L.; Quist, P.-O. A Novel Chiral Nematic Phase in Aqueous κ -Carrageenan. *Macromolecules* **1996**, *29*, 5926–5933.
- (38) Chronakis, I. S.; Ramzi, M. Isotropic-Nematic Phase Equilibrium and Phase Separation of κ -Carrageenan in Aqueous Salt Solution: Experimental and Theoretical Approaches. *Biomacromolecules* **2002**, *3*, 793–804.
- (39) Núñez-Santiago, M. d.C.; Tecante, A.; Garnier, C.; Doublier, J. L. Rheology and Microstructure of κ -Carrageenan under Different Conformations Induced by Several Concentrations of Potassium Ion. *Food Hydrocolloids* **2011**, *25*, 32–41.
- (40) Weiss, R. G.; Terech, P. Self-Assembled Fibrillar Networks. *Molecular Gels*; Springer-Verlag: Berlin/Heidelberg, 2006; pp 1–978.
- (41) Ako, K. Influence of Elasticity on the Syneresis Properties of κ -Carrageenan Gels. *Carbohydr. Polym.* **2015**, *115*, 408–414.
- (42) Nickerson, M.; Paulson, A. Rheological Properties of Gellan, κ -Carrageenan and Alginate Polysaccharides: Effect of Potassium and Calcium Ions on Macrostructure Assemblages. *Carbohydr. Polym.* **2004**, *58*, 15–24.
- (43) Takemasa, M.; Chiba, A.; Date, M. Gelation Mechanism of κ - and ι -Carrageenan Investigated by Correlation between the Strain-

Optical Coefficient and the Dynamic Shear Modulus. *Macromolecules* **2001**, *34*, 7427–7434.

(44) Sokolova, E. V.; Chusovitin, E. A.; Barabanova, A. O.; Balagan, S. A.; Galkin, N. G.; Yermak, I. M. Atomic Force Microscopy Imaging of Carrageenans from Red Algae of Gigartinaceae and Tichocarpaceae Families. *Carbohydr. Polym.* **2013**, *93*, 458–465.

(45) deGennes, P.-G. *Scaling Concepts in Polymer Physics*; Cornell University: New York, 1979.

(46) Rees, D. A.; Welsh, E. J. Secondary and Tertiary Structure of Polysaccharides in Solutions and Gels. *Angew. Chem., Int. Ed. Engl.* **1977**, *16*, 214–224.

(47) Dea, I. C.; McKinnon, A. A.; Rees, D. A. Tertiary and Quaternary Structure in Aqueous Polysaccharide Systems which Model Cell Wall Cohesion: Reversible Changes in Conformation and Association of Agarose, Carrageenan and Galactomannans. *J. Mol. Biol.* **1972**, *68*, 153–172.

(48) Oelschlaeger, C.; Cota Pinto Coelho, M.; Willenbacher, N. Chain Flexibility and Dynamics of Polysaccharide Hyaluronan in Entangled Solutions: A High Frequency Rheology and Diffusing Wave Spectroscopy Study. *Biomacromolecules* **2013**, *14*, 3689–3696.

(49) Burton, B. A.; Brant, D. A. Comparative Flexibility, Extension, and Conformation of Some Simple Polysaccharide Chains. *Biopolymers* **1983**, *22*, 1769–1792.

(50) Stokke, B. T.; Brant, D. A. The Reliability of Wormlike Polysaccharide Chain Dimensions Estimated from Electron Micrographs. *Biopolymers* **1990**, *30*, 1161–1181.

(51) Rees, D. A.; Scott, W. E. Polysaccharide Conformation. Part VI. Computer Model-Building for Linear and Branched Pyranoglycans. Correlations with Biological Function. Preliminary Assessment of Inter-Residue Forces in Aqueous Solution. Further Interpretation of Optical Rotation in T. *J. Chem. Soc. B* **1971**, 469–479.

(52) Owusu-Apenten, R. *Introduction to Food Chemistry*; CRC Press: Boca Raton, FL, 2005; p 249.

(53) Tanaka, F. *Polymer Physics*; Cambridge University Press, 2011; p 440.